

## Recurring mutations in *RPL15* are linked to hydrops fetalis and treatment independence in Diamond-Blackfan anemia

Marcin W. Wlodarski,<sup>1,2</sup> Lydie Da Costa,<sup>3,4,5,6</sup> Marie-Françoise O'Donohue,<sup>7</sup> Marc Gastou,<sup>3,4,8</sup> Narjesse Karboul,<sup>3,5</sup> Nathalie Montel-Lehry,<sup>7</sup> Ina Hainmann,<sup>1</sup> Dominika Danda,<sup>1,9</sup> Amina Szvetnik,<sup>1</sup> Victor Pastor,<sup>1,10</sup> Nahuel Paolini,<sup>11</sup> Franca M. di Summa,<sup>11</sup> Hannah Tamary,<sup>12,13</sup> Abed Abu Quider,<sup>14</sup> Anna Aspesi,<sup>15</sup> Riekelt H. Houtkooper,<sup>16</sup> Thierry Leblanc,<sup>17</sup> Charlotte M. Niemeyer,<sup>1,2</sup> Pierre-Emmanuel Gleizes<sup>7</sup> and Alyson W. MacInnes<sup>16</sup>

<sup>1</sup>Department of Pediatrics and Adolescent Medicine, Division of Pediatric Hematology and Oncology, Medical Center, Faculty of Medicine, University of Freiburg, Germany; <sup>2</sup>German Cancer Consortium (DKTK), Freiburg, Germany and German Cancer Research Center (DKFZ), Heidelberg, Germany; <sup>3</sup>University Paris VII Denis Diderot, Faculté de Médecine Xavier Bichat, Paris, France; <sup>4</sup>Laboratory of Excellence for Red Cell, LABEX GR-Ex, Paris, France; <sup>5</sup>Inserm Unit 1149, CRI, Paris, France; <sup>6</sup>Hematology Laboratory, Robert Debré Hospital, Paris, France; <sup>7</sup>LBME, Centre de Biologie Intégrative, Université de Toulouse, CNRS, UPS, France; <sup>8</sup>UMR1170, Gustave Roussy, Villejuif, France; <sup>9</sup>Department of Tumor Pathology, Centre of Oncology, Maria Skłodowska-Curie Memorial Institute, Poland; <sup>10</sup>Faculty of Biology, University of Freiburg, Germany; <sup>11</sup>Department of Hematopoiesis, Sanquin and Landsteiner Laboratory, AMC/UvA, CX Amsterdam, the Netherlands; <sup>12</sup>Hematology Unit, Schneider Children's Medical Center of Israel, Petach Tikva, Israel; <sup>13</sup>Sackler School of Medicine, Tel Aviv University, Israel; <sup>14</sup>Pediatric Hematology/Oncology Department, Soroka Medical Center, Faculty of Medicine, Ben-Gurion University, Beer Sheva, Israel; <sup>15</sup>Dipartimento di Scienze della Salute, Università del Piemonte Orientale, Novara, Italy; <sup>16</sup>Laboratory Genetic Metabolic Diseases, Academic Medical Center, Amsterdam, the Netherlands and <sup>17</sup>Pediatric Hematology Service, Robert-Debré Hospital and EA-3518, Université Paris Diderot - Institut Universitaire d'Hématologie, Paris, France

©2018 Ferrata Storti Foundation. This is an open-access paper. doi:10.3324/haematol.2017.177980

Received: August 4, 2017.

Accepted: March 6, 2018.

Pre-published: March 29, 2018.

Correspondence: marcin.wlodarski@uniklinik-freiburg.de

## SUPPLEMENTAL METHODS

**Pre-rRNA processing analysis.** Lymphoblastoid cell lines and HeLa cells were cultured in RPMI and DMEM, respectively (Gibco). These media were supplemented with 10% fetal bovine serum and 1 mM sodium pyruvate (Sigma). Different 19-mer siRNAs (Eurogentec, Seraing, Belgium), whose efficiency was verified by qPCR, were used to knock down expression of *RPL15* mRNA coding for eL15 protein in HeLa cells: eL15, siRNA eL15-1 (5'-UGGUGUUAACCAGCUAAAGdTdT-3') and siRNA eL15-2 (5'-UCCAGGAGCUAUGGAGAAAdTdT-3'). Each siRNA solution was added at a final concentration of 500 nM to 200  $\mu$ l of cell suspension ( $50 \times 10^6$  cells/ml diluted in sodium phosphate buffer, pH 7.25, containing 250 mM sucrose and 1 mM  $MgCl_2$ ). Electro-transformation was performed at 240 V with a Gene Pulser (Bio-Rad, Hercules, CA). (1) Control HeLa cells were electro-transformed with a scramble siRNA (siRNA-negative control duplex; Eurogentec). After 10 min incubation at ambient temperature, cells were plated and grown at 37°C for 48 hours.

**RNA extraction and analysis by northern blot.** Total RNAs were extracted with Trizol from cell pellets containing 20-30  $\times 10^6$  cells. The aqueous phase was further extracted with phenol-chloroform-isoamyl alcohol (25:24:1; Sigma), then with chloroform. Total RNAs were recovered after precipitation with 2-propanol. For Northern blot analyses, RNAs were dissolved in formamide, denatured for 10 min at 70°C and separated on a 1.2% agarose gel containing 1.2% formaldehyde and 1X Tri/Tri buffer (30 mM triethanolamine, 30 mM tricine, pH 7.9) (3  $\mu$ g RNAs/lane). RNAs were transferred to a Hybond N<sup>+</sup> nylon membrane (GE Healthcare, Orsay, France) by passive transfer. Pre-hybridization was performed for 1 hour at 45°C in 6X SSC, 5X Denhardt's solution, 0.5% SDS, 0.9 g/ml tRNA. The 5'-radiolabeled oligonucleotide probe was incubated overnight. The sequences of the probes were:

5'-ITS1 (5'-CCTCGCCCTCCGGGCTCCGTTAATGATC-3'),

ITS1-5.8S (5'-CTAAGAGTCGTACGAGGTCG-3'),

ITS2 (ITS2b: 5'-CTGCGAGGGAACCCCCAGCCGCGCA-3' and

ITS2d/e: 5'-GCGCGACGGCGGACGACACCGCGGCGTC-3'),

18S (5'-TTTACTTCTCTAGATAGTCAAGTTTCGACC-3'),

28S (5'-CCCGTTCCCTTGGCTGTGGTTTCGCTAGATA-3').

Membranes were washed twice for 10 min in 2X SSC, 0.1% SDS and once in 1X SSC, 0.1% SDS, and then exposed. Signals were acquired with a Typhoon Trio PhosphorImager (GE Healthcare) and quantified using the MultiGauge software.

**Polysome profiling analysis.** 400 $\mu$ g of total protein from freshly lysed LCLs or 1mg of total protein from freshly lysed HeLa cells were loaded onto 17-50% or 10-50% sucrose gradients, respectfully, as previously described.(2) The tubes were centrifuged at 4°C and at 40,000 rpm for 2 hours in a SW41 rotor (Optima L100XP ultracentrifuge; Beckman Coulter). The gradient fractions were collected at OD<sub>254</sub> with a Foxy Jr. gradient collector (Teledyne Isco).

**Growth curve.** 50,000 LCLs were plated in triplicate in a 12-well dish with DMEM +10%FCS and counted daily with a CASY® Cell Counter for five days. Each well was counted in triplicate each day. Statistics were performed with a Student's t-test.

**De novo protein synthesis measurement.** 100,000 LCLs were plated in 150 $\mu$ l methionine-free medium (DMEM containing 4.5g/L D-glucose, without L-glutamine, sodium pyruvate, L-methionine, and L-cysteine, Invitrogen

#21013). Assays performed using the Click-iT® AHA Alexa Fluor® 488 Protein Synthesis HCS Assay (Thermo Scientific) per the manufacturer's instructions using 2% paraformaldehyde for fixation and 1:1000 dilution of AHA. Fluorescence was measured by flow cytometry using an LSR-II apparatus and analyzed with FACSDiva software (BD Biosciences).

**TABLE S1**

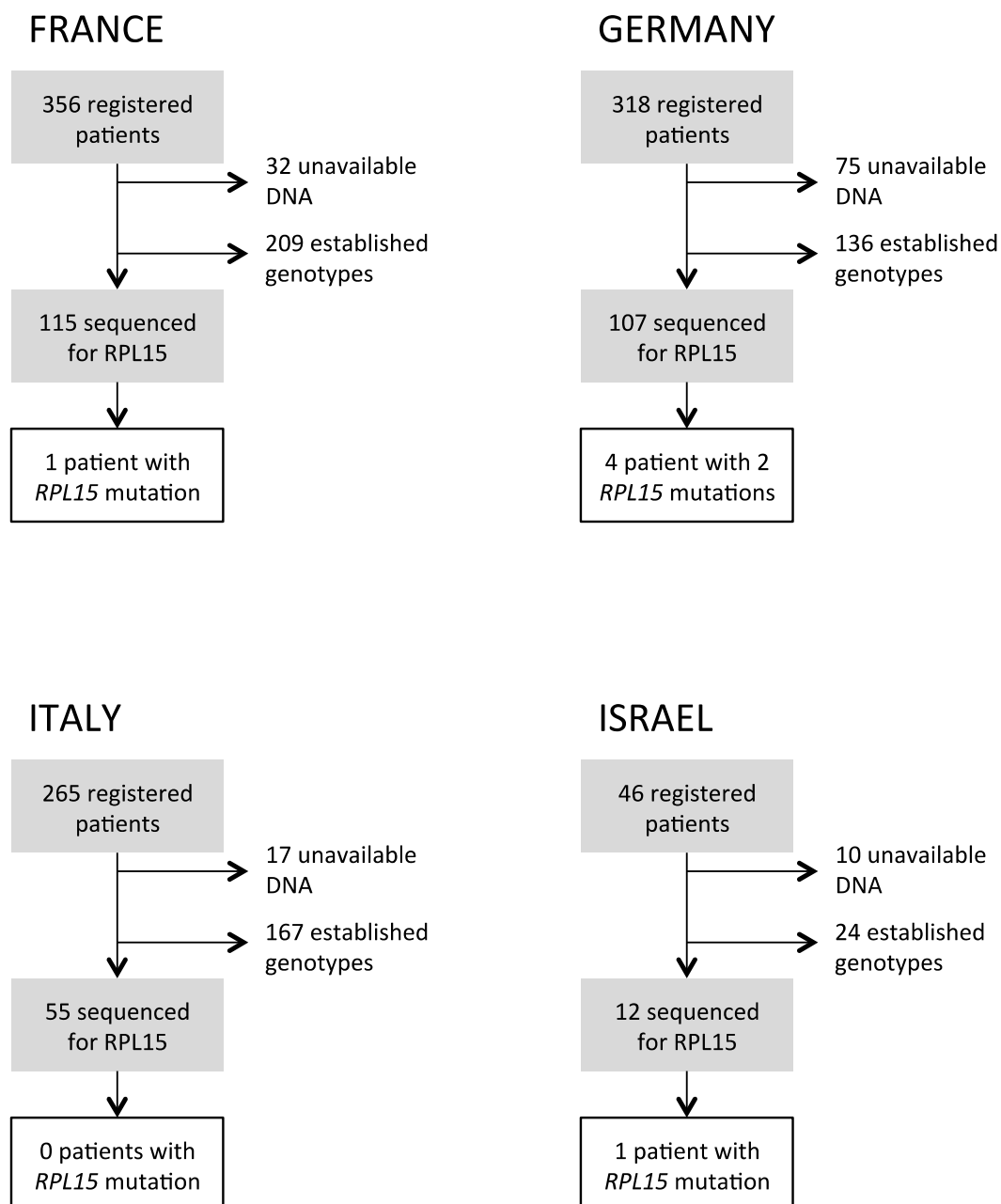
Patient	Genotype		Conservation / PhysChem.	Effect (SIFT/ MT/ PP2 / PSNP)	CADD	ExAC N°/ population
1-3	c.242dupA	p.Tyr81*	∅	Stop gain	25*	none
4	c.85C>T	p.Gln29*	∅	Stop gain	37	none
5	c.29T>C	p.Leu10Pro	High / Moderate	D/D/B/D	27	none
6	c.458A>C	p.Lys153Thr	High / Moderate	D/D/B/N	14	none

**Table S1. Evaluation of mutations in *RPL15* gene.**

Abbreviations: Conservation, evolutionary conservation scores using PhyloP and PhastCons; PhysChem., physicochemical difference between amino acids. *In silico* prediction: SIFT: D-deleterious; MT, Mutation Taster: D-disease causing; PP2, PolyPhen2: B- benign; PSNP consensus classifier: D-deleterious, N-neutral (% accuracy). CADD: Combined Annotation Dependent Depletion – score (method description: <http://cadd.gs.washington.edu/info>). A CADD score of 10 refers to the top 10% of deleterious variants detected in the human genome. CADD score above 20 represents the top 1% of deleterious variants. ExAC N°, number of heterozygous carriers; population, number of European individuals studied, as reported by Exome Aggregation Consortium ([exac.broadinstitute.org/](http://exac.broadinstitute.org/)). Gene annotation: *RPL15* (NM\_001253379).

\* Because the duplication of A nucleotide (c242dupA) in the Tyrosine-coding triplet (TAC → TAA A) did not yield a CADD score, we constructed the CADD score from nucleotide exchange TAC→TAA resulting in the same stop codon at position 81.

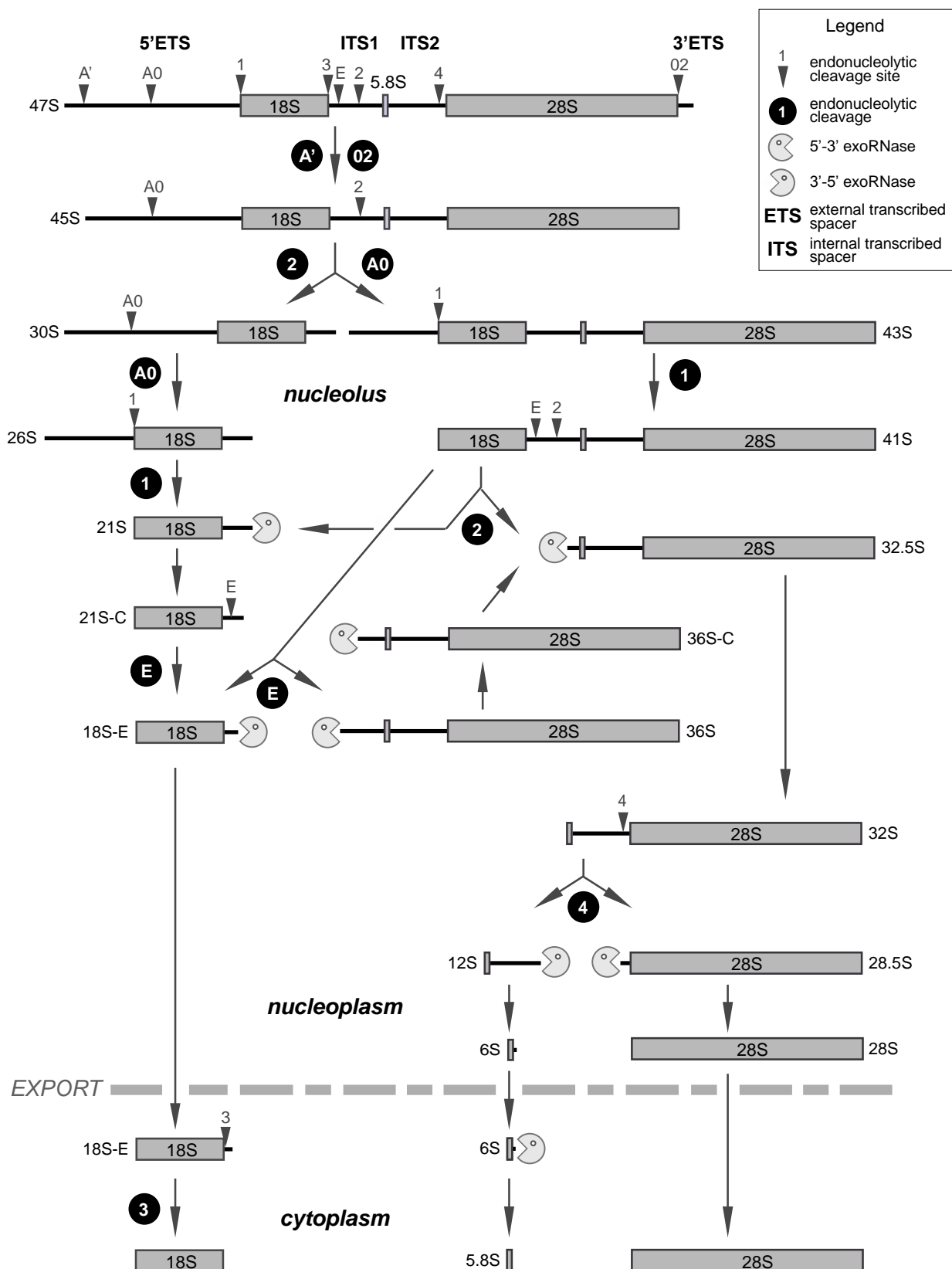
## FIGURE S1



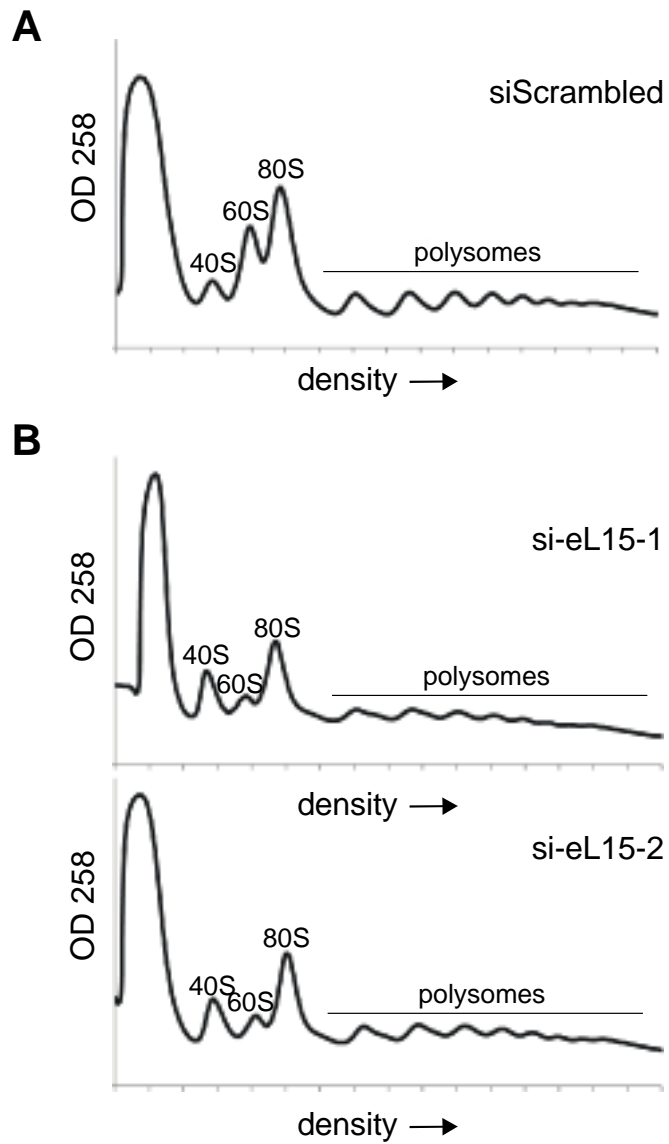
**Figure S1. Description of EuroDBA patient registries tested for RPL15 mutations.**

Four of the established registries within the EuroDBA consortium were included in this study. Numbers reflect calculations made in November 2017. In all cases, the cohorts tested for RPL15 mutations by Sanger sequencing consisted of registered patients with available DNA who had previously tested negative for mutations in all known DBA-linked genes.

**FIGURE S2**

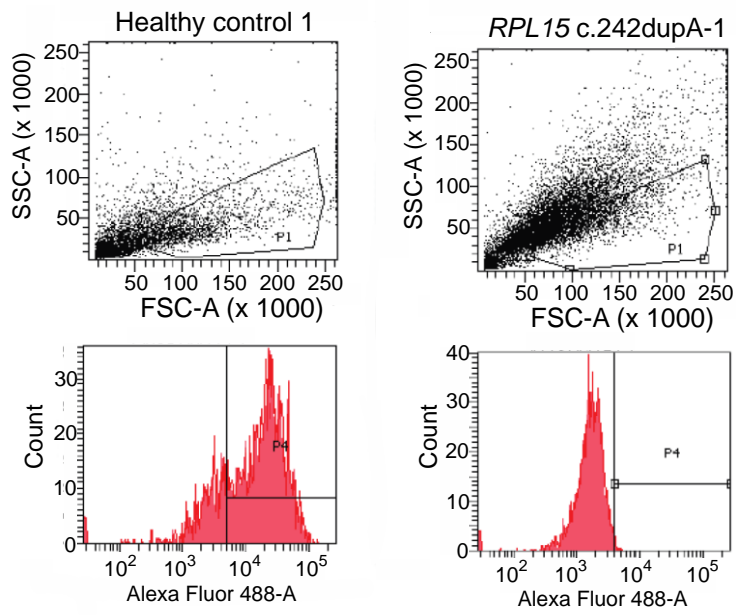


**Figure S2 (Related to Figure 3). A schematic of the pre-rRNA processing pathway in mammalian cells.**

**FIGURE S3**

**Figure S3 (Related to Figure 3). Polysome profiles of siRNA-treated HeLa cells.**

**A)** Profiles of HeLa cells treated with a scrambled siRNA. **B)** Profiles of HeLa cells treated with two siRNAs against eL15 (*RPL15*). 40S subunits, 60S subunits, 80S monosomes, and polysomes are labeled.

**FIGURE S4**

**Figure S4 (Related to Figure 4). FACS plots of AHA labeling of LCLs for de novo protein synthesis measurements.**

**A)** Plots of LCLs from a healthy control. **B)** Plots of LCLs from an individual with a *RPL15* mutation.



**FIGURE S5**

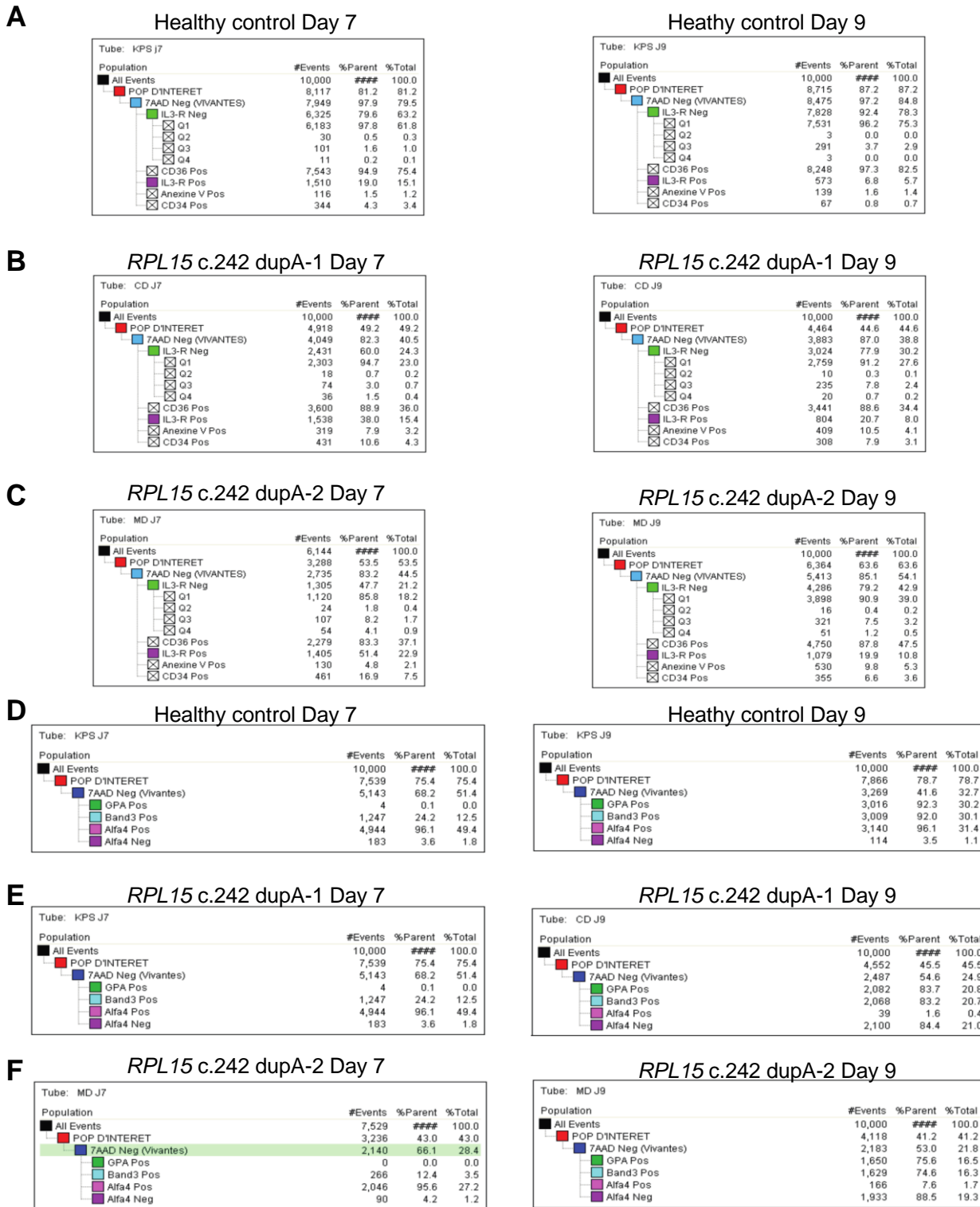


**Figure S5 (Related to Figure 5). FACS results of red cell culture assays. A)** Results from blood sample from a healthy control on days 7 and 9, Annexin V, CD34<sup>+</sup>, and CD36<sup>+</sup> staining. **B)** DBA patient carrying the mutation *RPL15* c.242 dupA-1 on days 7 and 9, Annexin V, CD34<sup>+</sup>, and CD36<sup>+</sup> staining. **C)** DBA patient carrying the mutation *RPL15* c.242 dupA-2 on days 7 and 9, Annexin V, CD34<sup>+</sup>, and CD36<sup>+</sup> staining. **D)** Results from blood sample from a healthy control on days 7 and 9, Band-3+ and Alpha-4+ staining. **E)** DBA patient carrying the mutation *RPL15* c.242 dupA-1 on days 7 and 9, Band-3+ and Alpha-4+ staining. **F)** DBA patient carrying the mutation *RPL15* c.242 dupA-2 on days 7 and 9, Band-3+ and Alpha-4+ staining.

## References

1. Paganin-Gioanni A, Bellard E, Escoffre JM, Rols MP, Teissie J, Golzio M. Direct visualization at the single-cell level of siRNA electrotransfer into cancer cells. *Proceedings of the National Academy of Sciences of the United States of America*. 2011 Jun 28;108(26):10443-7.
2. Pereboom TC, van Weele LJ, Bondt A, MacInnes AW. A zebrafish model of dyskeratosis congenita reveals hematopoietic stem cell formation failure resulting from ribosomal protein-mediated p53 stabilization. *Blood*. 2011 Nov 17;118(20):5458-65.